CLM - R 142

UKAEA RESEARCH GROUP

Report

STUDIES OF THE MAGNETIC CONFIGURATION OF AN ℓ=2 STELLARATOR

O I FEDYANIN

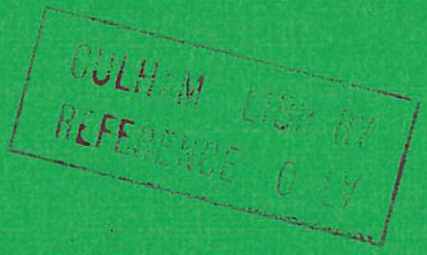

CULHAM LABORATORY
Abingdon Oxfordshire
1975

Available from H. M. Stationery Office

C.18

PRICE £1.00

U.D.C.
621.039.623 PROTO-CLEO : 538. 122
621.039.667.4

CLM - R 142

STUDIES OF THE MAGNETIC CONFIGURATION OF AN ℓ=2 STELLARATOR

by

O.I. FEDYANIN

(attached from Lebedev Institute, Moscow, under Royal Society auspices)

'EURATOM - U K A E A Fusion Association, Culham Laboratory, Abingdon, Oxon, OX 14 3 DB, U.K.'

A B S T R A C T

The first part of this report describes a computational study of the effect of first and second order resonances on an $\ell = 2$ stellarator, taking as a model the PROTO-CLEO experiment. The magnetic surfaces are computed in each case and the break up shown. The second part of the report deals with measurements made with an electron beam on the PROTO-CLEO $\ell = 2$ stellarator. The magnetic surfaces are measured by means of a movable probe which intercepts the beams. It is shown that the form of the surfaces, particularly near the separatrix, is sensitive to quite small perturbations of a resonant type.

May, 1975

SBN: 85311 035 2

STUDIES OF THE MAGNETIC CONFIGURATION OF AN $\ell = 2$ STELLARATOR

by

O. I. FEDYANIN

Editor's Note

The work described here was carried out by the author while on attachment to the Culham Laboratory from the Lebedev Institute, Moscow. It originally received limited circulation as internal memoranda. It is felt, however, that it deserves wider circulation and it is thus being published in report form. The report is in two parts. Part I describes computations carried out to determine the magnetic surfaces at resonant conditions for a stellarator of PROTO-CLEO dimensions, while Part II is concerned with electron beam measurements on the PROTO-CLEO apparatus to determine the magnetic surfaces.

PART I

RESONANCES IN AN $\ell = 2$ STELLARATOR

Studies of plasma confinement in stellarators have shown how strongly this is influenced by magnetic field structure (see the work of the Lebedev Institute group and Garching group).

It is possible to list two reasons for this influence. First, the change of plasma size - diffusion length, which of course does not influence the diffusion of plasma, but decreases the decay time. Second, magnetic field lines are closed after one or more revolutions, which produces the optimum reason for excitation of a longitudinal plasma instability.

For these reasons a knowledge of magnetic structure and the sensitivity of this structure to a perturbation is a very desirable thing.

The methods of determination of the magnetic structure are relatively simple ones. It is possible to obtain an analytic distribution by using the Fourier components of magnetic field and also to calculate the trajectory of a magnetic line by using a computer. (Usually in this method the magnetic field is determined from the Bio-Savart equation.)

The analytic method becomes more complicated for large toroidicity and the existence of a resonant perturbation. Computation of a magnetic structure remains the same in principle. The period of the structure changes in this case; whereas for the basic structure a period is equal to a helical field period, the main role for the determination now is governed by the perturbation. As an example, for the first and second resonances $\tau = 1$ and $\tau = 0.5$ the period equals the torus perimeter.

A computer program TORFLD was used to calculate the shape of the magnetic surfaces.

The calculation has been carried out for the main resonances: $\tau_1 = 1$ and $\tau_2 = 0.5$.

The resonance perturbations for $\tau = 1$. The perturbations, which have the following expression for magnetic potential:

$$F = F_0 r \, As \, (\theta - \frac{z}{R} + F)$$

r - minor radius of torus (see Fig.1)

R - major radius of torus

$Z = R \cdot \varphi$, ψ - phase;

are resonant for $\tau = 1$.

Examples of such perturbations are the mutual displacement of the toroidal and helical fields, a mutual tilt, elliptical helical axis, uniform horizontal field, whose vector is in the main plane of the torus etc.

All perturbations have the form of standing waves, but decomposition of such a one gives two travelling waves, one of which is the resonance wave for a helical field. The opposite travelling wave is neglected.

For example the magnetic potential of a horizontal field is

$$F = B^{(\tau)}_r \cos\theta \cos \frac{z}{R}$$

or

$$F = \frac{B^{(\tau)}_r}{2} \cos\left(\theta - \frac{z}{R}\right) + \cos\left(\theta + \frac{z}{R}\right)$$

Resonance harmonics could be either, but this depends on the law of the helix: right or left handed. A horizontal field has been used to produce the perturbation field.

The field produced by a magnetic quadrupole has been chosen to excite a resonance perturbation for the $\tau = 0.5$ case.

A magnetic quadrupole has two current carrying coils with opposite magnetic senses (see Fig.2).

The following parameters have been used for the computation:

Major radius of the torus	$R = 40$ cm
Radius of the helix	$A = 9.3$ cm
Multiplicity	$\ell = 2$
Number of field periods	$n_{fp} = 6$
Helix current ($\tau = 1$)	$I\ell = 20$ kA
Helix current ($\tau = 0.5$)	$I\ell = 14.3$ kA
Equivalent straight line current to produce $B\varphi$ ($\tau = 1$)	$I_\varphi = (6.2\text{-}5.94)10^2$ kA
Horizontal magnetic field	$B_h = 3G$; $\left(\frac{B_h}{B_\varphi} = 3 \times 10^{-3}\right)$
Radius of quadrupole coils	$r_o = 10$ cm
Distance to main plane of torus	$b_o = \pm 10$ cm
Quadrupole current	$I_K = 2$ kA

Magnetic surfaces for the second resonance ($\tau = 0.5$). The structure which has been chosen for the investifation is shown on Fig.3 (perturbation field absent).

The degenerate surface $\tau = 0.5$ is placed between $1(\tau_1 = 0.463$ and $2(\tau_2 = 0.630)$. If a perturbation is present, the shape of the complete surfaces is changed. The new shapes are shown in Fig.4.

The resonance structure has two magnetic axes, one is circular, but the other is helical whose radius equals approximately the radius of the degenerate surface and the law of the helix is $2\theta = \varphi$.

This geometry has three groups of surfaces: one surrounds the circular axis, the second - helical one, the third - both axes. The numbers in Fig.4, designate the number of revolutions. The shape of the magnetic surfaces is demonstrated for the different position of the basic one ($\varphi = 0$, $\varphi = 45$).

Structure for the first resonance ($\tau = 1$). The variation of magnetic structure has been investigated in detail for this case. The shape of an internal magnetic surface and the dependence of average angle of rotation on the straight line current (or parameter ε) are shown in Fig.5. The variation of the relative perturbation is negligible.

Figs.6 and 7 show magnetic surfaces in the presence of a resonant perturbation. The main parameter is I_φ current. We now consider the evolution of the shapes with variation of angle of rotation ($\tau(r = 0)$ increases, if I_φ decreases). The initial magnetic axis is a circle for which the equation is $\theta = \text{constant}$, $r = \text{constant}$.

In presence of a perturbation the magnetic axis is split into two helical ones (O_1 and O_2) for which the equation is $\theta = \varphi$.

For the larger $\tau(0)$ (or $I_\varphi = 620 \div 610$), but $\tau(0) \sim 1$, there is only one helical magnetic axis. A new group of surfaces is beginning to form around O_2. The dotted lines of Figs.6 and 7 show

'disclosed surfaces', but the magnetic line has still 10 rotations. Two axes O_1 and O_2 exist for the current $I_\varphi = 6.05$. There are three groups of surfaces in the similar case of secondary resonance (but helical axes).

If $\tau(0)$ increases, surfaces which surround the 'old' axis, finally disappear. For the current $I > 5.93$ the magnetic structure has only one 'new helical' magnetic axis O_2.

Figure 8 shows the rotation of the magnetic surfaces and axes. The shape of the surfaces for every period of the field are shown. It is possible to see that the magnetic surfaces rotate 180 degrees in three field periods.

It should be interesting to compare the results of computation and experimental data, but magnetic measurements on PROTO-CLEO have been carried out only for the resonance $\tau = \frac{1}{3}$. For instance, it is possible to demonstrate the resonance structure of the magnetic field of the stellarator TOR-1 which occurs in these cases (Fig.9). A broad view of the structure shows they are very similar. But it is possible to see only qualitative agreement, because the parameters of the magnetic field are very different in the two cases.

PART II

MEASUREMENTS ON THE MAGNETIC FIELD STRUCTURE OF PROTO-CLEO ($\ell = 2$)

The main studies of plasma confinement in the PROTO-CLEO stellarator have used the $\ell = 3$ field windings but for comparison, confinement studies have also been carried out using the $\ell = 2$ system.

The $\ell = 2$ helical magnetic field is generated by four equally spaced helical conductors. Each conductor conforms to the curve $\theta = N\varphi$ where θ is the azimuthal angle in the equatorial plane, φ is the angle between the helix radius and the major plane of the torus, and N is a small integer.

The geometrical parameters of the helical windings are:

Major radius of the torus	$R = 40$ cm
Radius of the helix	$a_o = 9.3$ cm
Diameter of a single conductor	$r = 1.2$ cm
	$N = 3$
Helix pitch	$L = 83.7$ cm.

The helical windings and the coils for producing the toroidal field were energised from capacitor banks. By varying the ratio of currents in the two field systems, it was possible to change the value of ϵ_2, which is the ratio of the amplitude of the main harmonic of the helical field to the toroidal field. For the fixed geometrical dimensions of the system, ϵ_2 is the main parameter, in the absence of higher harmonics, ϵ_4, ϵ_6 ... etc, which defines the structure of the magnetic field in a stellarator.

Method of Magnetic Measurements

The way in which the magnetic measurements, used for studying the structure of the field of a magnetic trap, are carried out has been described in a series of articles[1-3]. Briefly, the method is as follows.

As the motion of electrons in a strong magnetic field can be described sufficiently accurately by the drift surface of the electron beam, then a study of the geometry and the motion of the electrons occupying the drift surfaces leads to an understanding of the structure of the field. The drift surfaces differ from the magnetic surfaces by an amount equal to the order of the Larmor radius in the helical field, i.e. are displaced[4] by a value Δr

$$\Delta r = \frac{2\pi}{i} \frac{v_{\parallel}^2 + \frac{1}{2} v_{\perp}^2}{\omega_{eB} v_{\parallel}} \simeq \frac{\rho_{eB}}{\dot{t}} \qquad \ldots (1)$$

where $\dot{t}$ is the rotational transform angle of the system $\left(\dot{t} = \frac{i}{2\pi}\right)$, ω_{eB} is the Larmor frequency, $v_{\parallel}$ and $v_{\perp}$ are the velocity components relative to the direction of the field, ρ_{eB} is Larmor radius.

An electron gun is introduced producing a pulse of electrons, which travel along the surfaces. Detection of the beam was carried out using a local probe.

The electron beam used in PROTO-CLEO possessed the following parameters:

Electron energy	$W_e \simeq 25$-27 eV
Pulse length	$t \simeq 1.2$ μsec
Beam width	~ 0.5-1 mm
Beam current	$I_e \sim 5$-10 μamps.

The local probe is a disc 1.5 mm in diameter, electrostatically screened; the screen can be used also for measurement of the beam. The probe measured the value of the charge $\left(q = \frac{1}{c}\int j(t)\, d\, Sdt\right)$, passing across a fixed point in space and traversed every point of the vacuum chamber. The coordinates of the probe system could be correlated with the geometry of the helical windings in the chamber where the magnetic measurements were carried out.

Fig.10 shows the schematic circuit for the power supply of the electron beam source and the circuit which is used for the local probe.

Measurements were carried out with the value of the magnetic field B in the range 1.2 - 1.5 kG and the angle of rotation τ varying between 0.3 and 1.0. With these parameters, the maximum value of the displacement of the drift surface relative to the magnetic surface did not exceed 0.5 mm.

Results of the Magnetic Measurements

The magnetic measurements determined the structure of the magnetic surfaces for a constant value of the toroidal field with two values of the helical winding current and defined the boundary magnetic surface. These results were compared with the calculated values.

One of the main characteristics of the helical field is the dependence of the rotational transform on the radius, the angle of the rotational transform for an $\ell = 2$ system is given by the following expression[4]

$$\tau = 2\pi R\alpha \left[1 - (1-\epsilon^2)^{\frac{1}{2}} + (\alpha r)^2 \frac{\epsilon^2(1+\epsilon^2)}{(1-\epsilon^2)^{\frac{3}{2}}} \right] \qquad \ldots (2)$$

where r is the mean radius of the magnetic surface parameter $\alpha = \frac{2\pi}{L} = \frac{N}{R}$.

For $(\alpha r)^2 \ll 1$ the dependence of τ on r can be neglected. The dependence of the angle of the rotational transform on ϵ and the corresponding helical winding current is shown in Fig.11. The curve is derived from the analytic expression (2) and the points are computed using the TORFLD program.

The angle of the rotational transform, $\underline{\tau}$, is determined by measurements of the coordinates of the electron beam for the first few identifiable revolutions.

Usually it is possible to identify 10 to 12 revolutions. In Fig.12 is shown an oscillogram signal from the probe in which it is possible to observe up to 9 revolutions of the beam.

In order to determine the average value $\langle \tau \rangle$ it is necessary to take into account the oscillating part of the angular rotation. The complete expression for the angular coordinate of a magnetic line is:

$$\theta = 2\pi\omega \frac{Z}{L} - \varepsilon \frac{1}{\underline{\rho}^2} I_2(2\rho) \sin 2\psi \qquad \ldots (3)$$

when

$$\omega = 1 - (1-\varepsilon^2)^{\frac{1}{2}} + \underline{\rho}^2 \frac{\varepsilon^2(1+\varepsilon^2)}{(1-\varepsilon^2)^{\frac{3}{2}}}$$

$$\psi = (\omega - 1)\alpha Z \qquad Z = R\varphi$$

or for $2\rho \ll 1$, $\varepsilon^2 < 1$, $\frac{\rho}{\underline{\rho}} \approx 1$, $z_j = NLj$

when $j = 0, 1, 2 \ldots\ldots$

$$\theta_j = 3\pi\varepsilon^2 j - \frac{\varepsilon}{2} \cos 6\pi\varepsilon^2 j ,$$

or $$\theta_j = \langle \tau \rangle_j - \frac{\varepsilon}{2} \cos \langle \tau \rangle_j .$$

If the oscillation is not taken into account in the measurement of $\langle \tau \rangle$ there is an error which decreases as the number of revolutions increases.

The experimentally determined value of the average angle of rotation is given by

$$\langle \tau \rangle = \frac{\theta_j^{exp} - \theta_o^{exp}}{j} \left(1 \pm \frac{\varepsilon + \Delta\theta^{exp}}{\theta_j^{exp} - \theta_o^{exp}} \right) \qquad \ldots (4)$$

where j is the number of revolutions;

θ_o^{exp} is the initial angle;

θ_j^{exp} is the angle of the j revolution;

$\Delta\theta$ is the error in determining the angle.

A typical form of the magnetic surfaces is shown in Fig. 13 for various numbers of revolution of the electron beam, and the figure shows the average value of the angle of rotation. The corresponding values of ε determined from the diagram are equal to $\varepsilon_1 = 0.445$, $\varepsilon_2 = 0.518$ $(\underline{\tau} = 0.43)$.

The magnetic surface of the $\ell = 2$ stellarator, corresponds as a first approximation, to an ellipse and can be described by the equation

$$X^2 \left[1 - \varepsilon \cos 2(\alpha - dz)\right] = X^2 \qquad \ldots (5)$$

where

$$X = 2\alpha r \ , \qquad \alpha = \frac{2\pi}{L}$$

From this equation the relation between r_{max}, r_{min} and r_{cp} can be seen

$$r_{max} \cdot r_{min} = \frac{r}{\sqrt{1 - \varepsilon^2}}$$

From the experiment τ, r_{max} and r_{min} can be determined, and ε, r and the shape of the magnetic surface can be calculated. In Fig.13, the dotted line shows the calculated magnetic surface.

The value for the displacement of the magnetic axes towards the centre of the torus is in good agreement with computer calculations and equals $\sim 4.5 - 5.0$ mm.

Comparison of the analytical result and the results of computer calculations are in good agreement also for $X_{max} = 2\alpha r < 0.2 - 0.3$.

The first main problem in making the magnetic measurements is to establish if in fact closed magnetic surfaces exist in the stellarator; this has been done. The second problem is to determine the actual working region, for the parameter ε or the helical current, for a constant toroidal field.

This problem is associated with the fact that the stellarator has a resonance range, i.e. the angle of the rotation transform $\tau = p/q$. $(p, q, = 1, 2, 3, \ldots)$. This resonance is due to the coincidence of the moving point with the initial position, after one or more revolutions (orbits).

The existence of such a resonant, 'τ' is not dangerous, but the presence of many perturbations, i.e. perturbations around the minus axis of the torus, toroidal and axial perturbations of the toroidal and helical fields, displace the toroidal helical magnetic fields, distort the magnetic surfaces, and shift the magnetic axis to give rise to formation of 'island structures'.

Measurement of the outer magnetic surfaces for PROTO-CLEO, for two cases $I = 12\,kA$ ($\epsilon = 0.445$) and $I = 14\,kA$ ($\epsilon = 5.518$), show the existence of a resonance perturbation structure in the stellarator. (see Figs. 14, 15).

Detailed measurements have been made initially for the case $\epsilon = 0.445$. This can be characterised by the third resonance $\tau = \frac{1}{3}$. The radius of the central islands are in agreement with a value derived from the angle of rotation. From the size of the island, the value of the harmonic of the perturbing field can be estimated[4], which scalar potential has an equation of the form

$$\varphi = \varphi_o z^n \cos(3\varphi - \frac{z}{r} + \varphi) \quad n > 1 \qquad \ldots (6)$$

φ is the phase of the perturbation,

$$\frac{\Delta\beta}{B} = \frac{m\epsilon^2}{\delta} X_{res}^2 \left(\frac{\Delta X}{X_{res}}\right)^2 \qquad \ldots (7)$$

$\Delta\beta$ = amplitude of the harmonic
m = 3, number of resonance
ΔX = size of island

$$\frac{\Delta X}{X} \simeq \frac{1}{5} - \frac{1}{7} \qquad r_p = 3.5\,cm$$

$$\frac{\Delta B}{B} \simeq (1-2) \times 10^{-5}$$

Hence it follows that the PROTO-CLEO field is sensitive to resonance perturbations.

The second case (see Fig.15), corresponds to 2nd resonance (represented by the dotted line in Fig.15, the structure of the field calculated by the computer). In this case, the detailed structure of the magnetic surface was not determined. However, by comparing with computer calculations, it is possible to observe a distortion of an outer magnetic surface. In the distorted magnetic surface two islands appear, typical of the second resonance. For instance, it is possible to show an island structure similar to the magnetic field of the stellarator TOR-1 which occurs in this case (Fig.9).

The present resonant structure of the field of PROTO-CLEO makes it difficult to define the boundary surface in this case. In both cases the boundary of the magnetic surface moves 2-3 mm in the direction of the main radius.

CONCLUSIONS

The magnetic field structure of PROTO-CLEO ($\ell = 2$) winding is a very interesting one for plasma physics experiments. All that is necessary is to calculate precisely the computed values. It is necessary to determine the exact position of the unperturbed regions of the magnetic structure because the magnetic field is very sensitive to perturbations.

ACKNOWLEDGEMENT

The work in Part II was carried out in collaboration with B.J. Parham.

APPENDIX

During the recording of the magnetic measurements a change in the angle of rotation was detected. For example, the signal from the probe measuring the 2nd or 3rd revolution was interrupted after a few shots. Special measurements showed that this was possibly due to the movement of the electron beam after 10-15 shots using the apparatus. The effect is connected with the heating of the helical winding and the divertor, changing the current relationships.

The temperature coefficient of resistance of copper $\alpha = 4 \times 10^{-3}$, i.e. if the temperature changes by 10°, the resistance changes by 4%, e.g. $\tau \simeq CI^2$; $\frac{\Delta\tau}{\tau} \simeq 0.1$, i.e. the value of the angle of rotation moves slowly along the minor radius. In the resonant case the magnetic structure is very sensitive to its effect.

Considerable difficulty arose in determining the resonant structure in the third resonance case, because in this case the field structure changed from shot to shot.

REFERENCES

(1) BEREZHETSKY, M.S., GREBENSHCHIKOV, S.E., POPRYADUKHIN, A.P. and SHPIGEL, I.S., Zh. Tech. Fiz., 35, 12 (1965) 2167.

(2) ANDRYUKHINA, E.D., FEDYANIN, O.I. and KHOLNOV, Yu.V., Preprint of the Lebedev Physics Institute 118 (1969); Proceedings of the Lebedev Physics Institute of the USSR Academy of Sciences (1971).

(3) IVANOVSKY, M.S., POPOV, S.N. and POPRYADUKHIN, A.P. in Collection: 'Plasma Confinement in Stellarators', USSR Acad. Sci. Phys. Inst., Preprint 94, Moscow (1968), 42.

(4) SOLOVEV, L.S. and SHAFRANOV, V.D., Problems in Plasma Theory, 5, Atomizdat (1967).

DANILKIN, I.S. and KARPENKO, I.K., Preprint of the Lebedev Physics Institute of the USSR Academy of Sciences, 114, (1967).

MOROZOV, A.I. and SOLOVEV, L.S., Problems in Plasma Theory, 2, Gosatomizdat (1963) (in Russian).

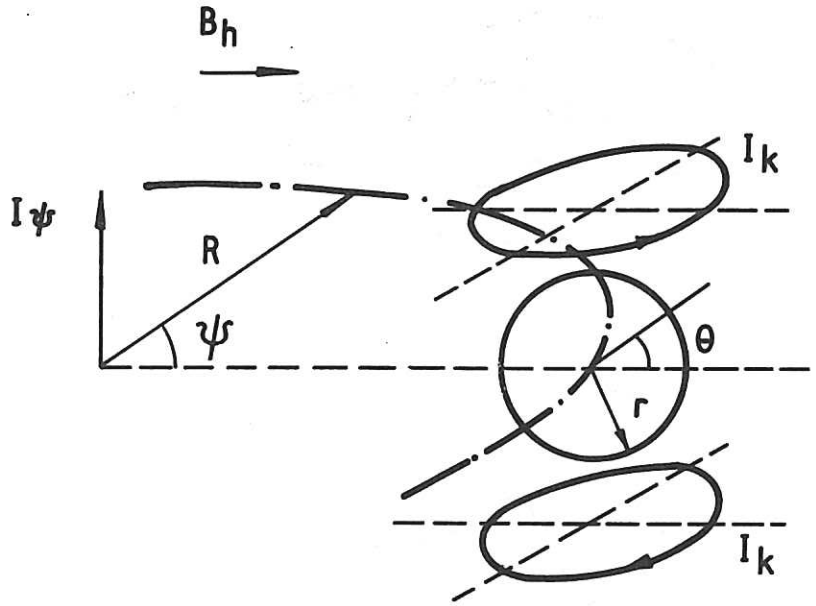

Fig.1 and Fig.2 The magnetic field configuration shown with possible perturbations.

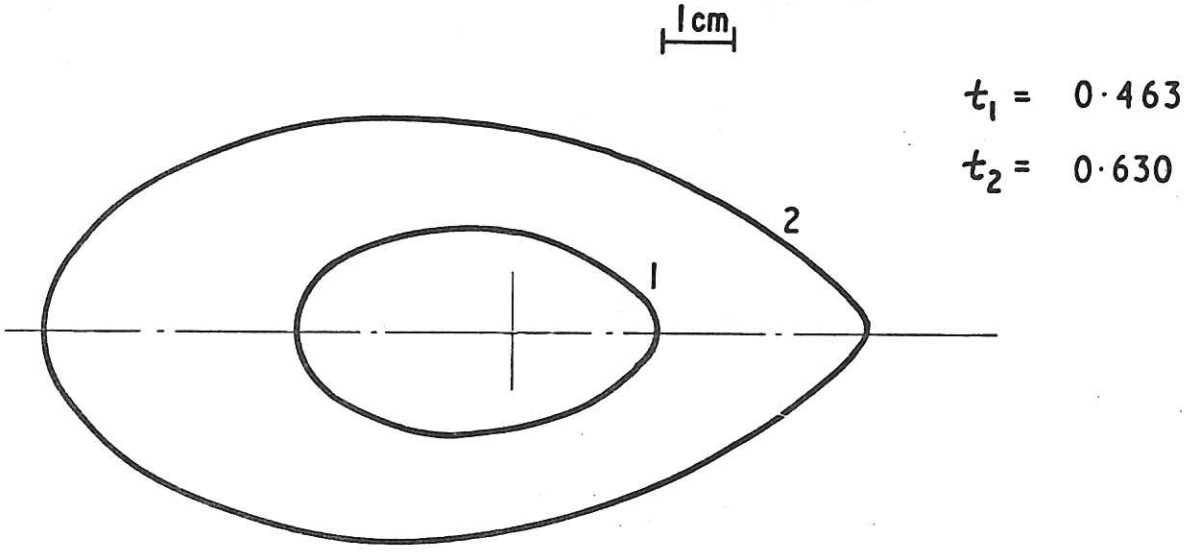

Fig.3 Resonance of the second kind ($\iota = 0.5$). Unperturbed surface.

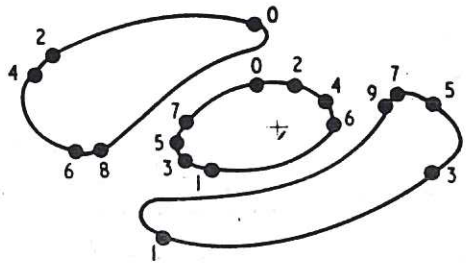

$\psi = 0°$

$t = 0.5$

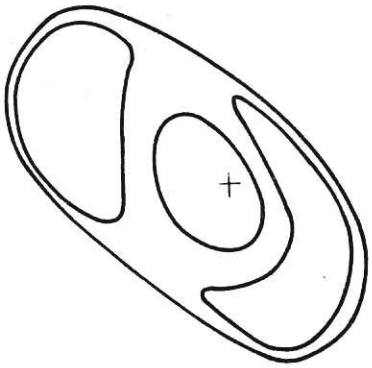

$\psi = 45°$

1cm

Fig.4 Resonance of the second king ($t = 0.5$). Perturbed surfaces.

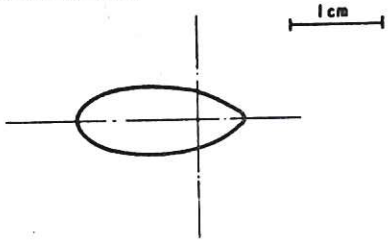

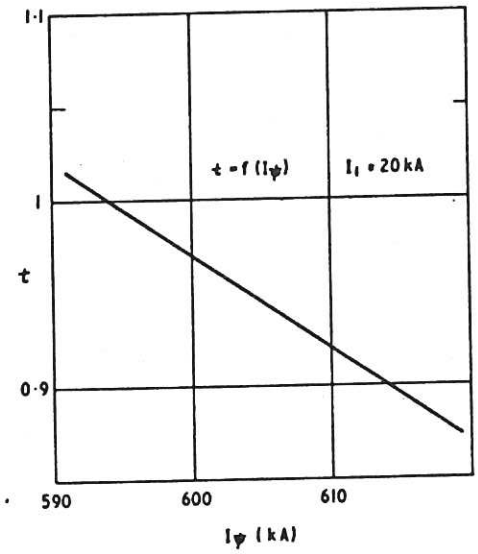

Fig.5 Resonance of the first kind ($t = 1$). Unperturbed surface and dependence of t on $I\Psi$ (line current generating B_ϕ).

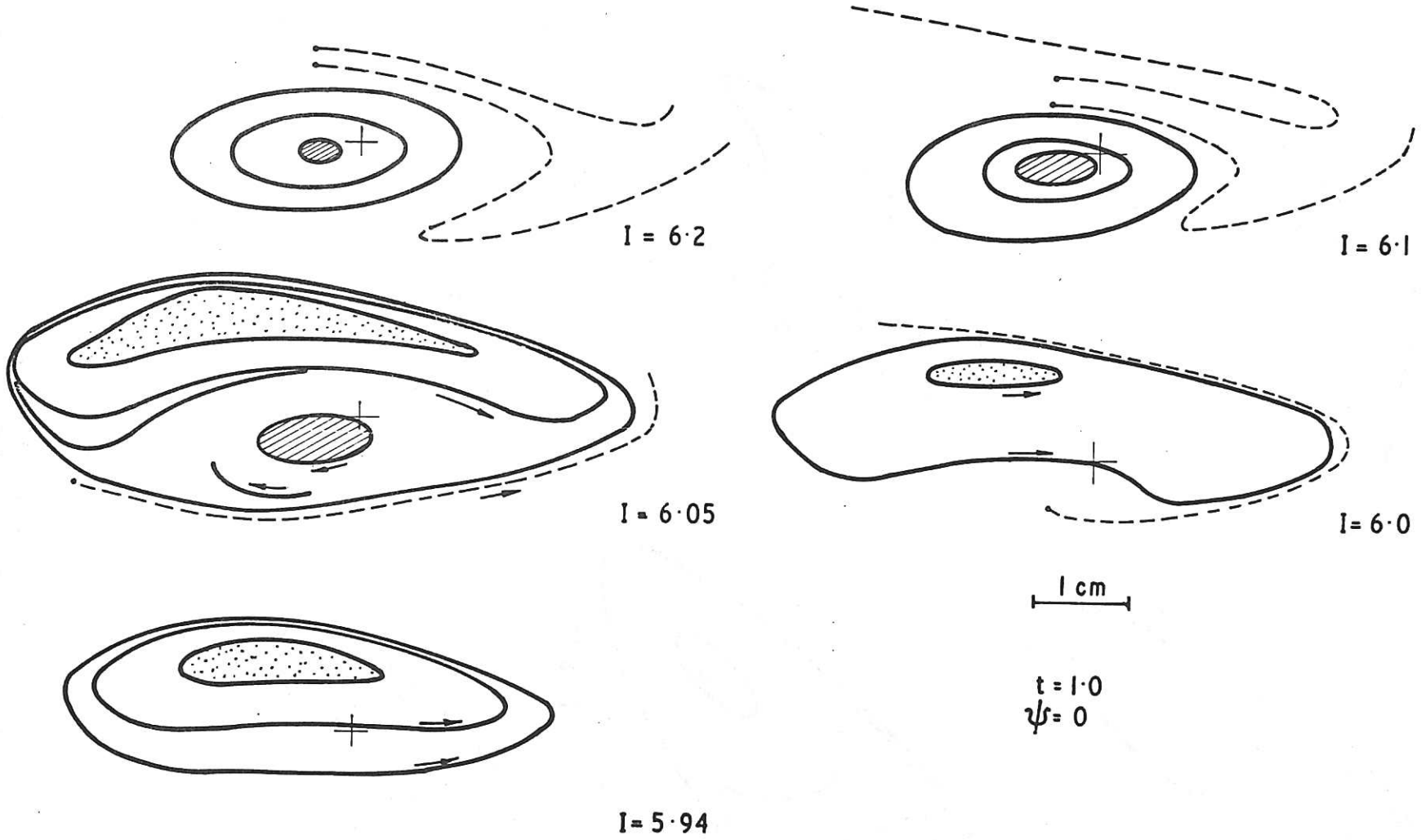

Fig.6 Resonance of the first kind ($\epsilon = 1$). Perturbed surfaces $\Psi = 0$.

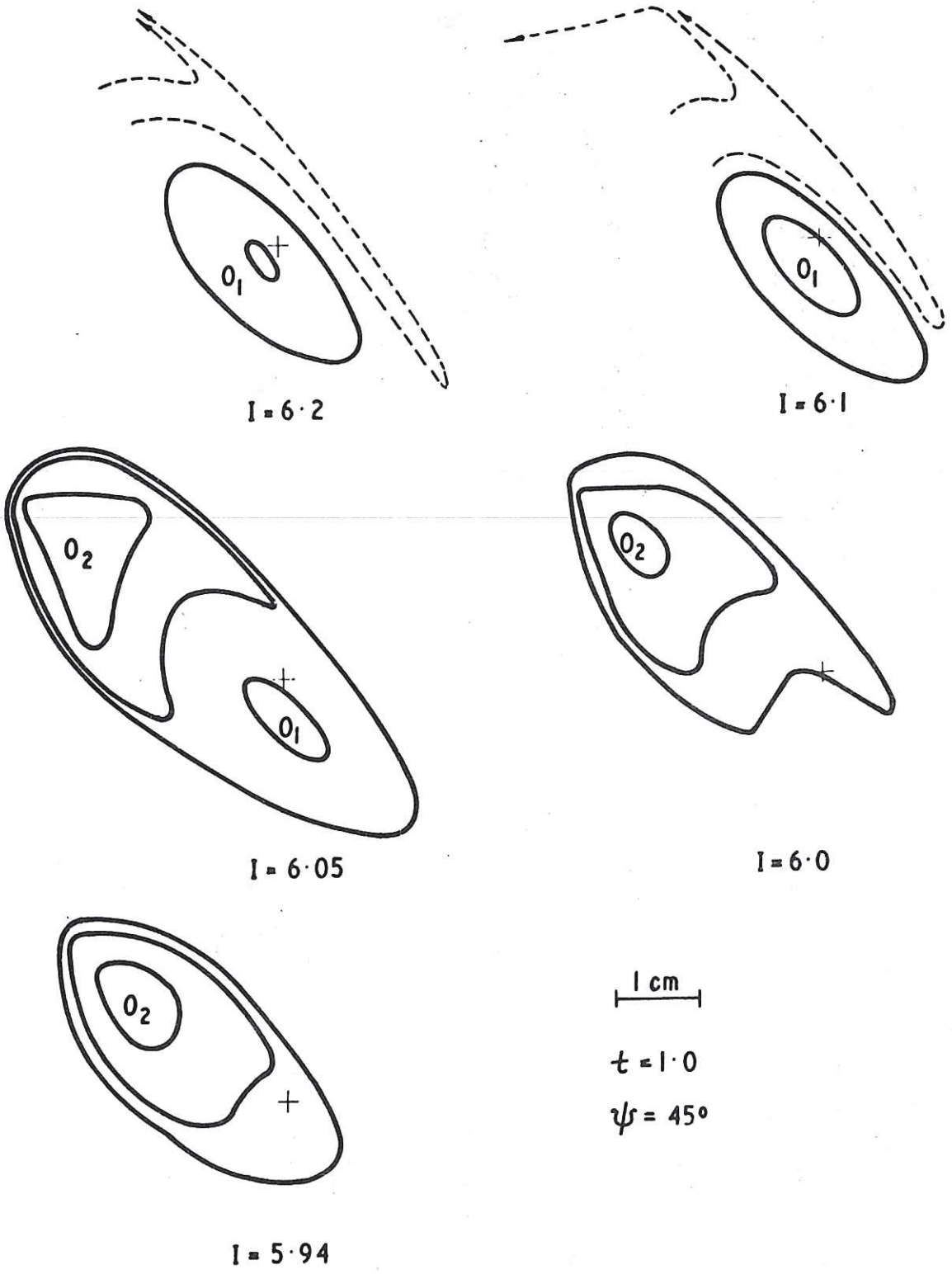

Fig.7 Resonance of the first kind ($t = 1$).
Perturbed surfaces at $\Psi = 45^{o}$.

CLM - R 142

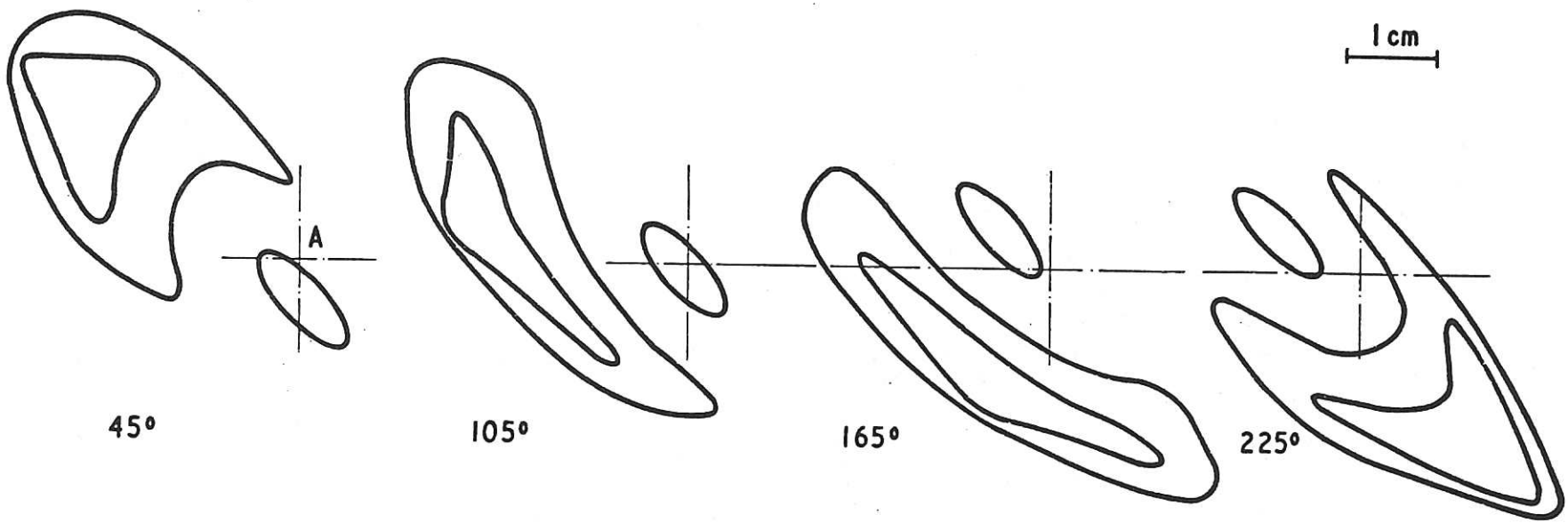

Fig.8 Resonance of the first kind ($\iota = 1$). Perturbed surface as a function of position in the major azimuth (Ψ).

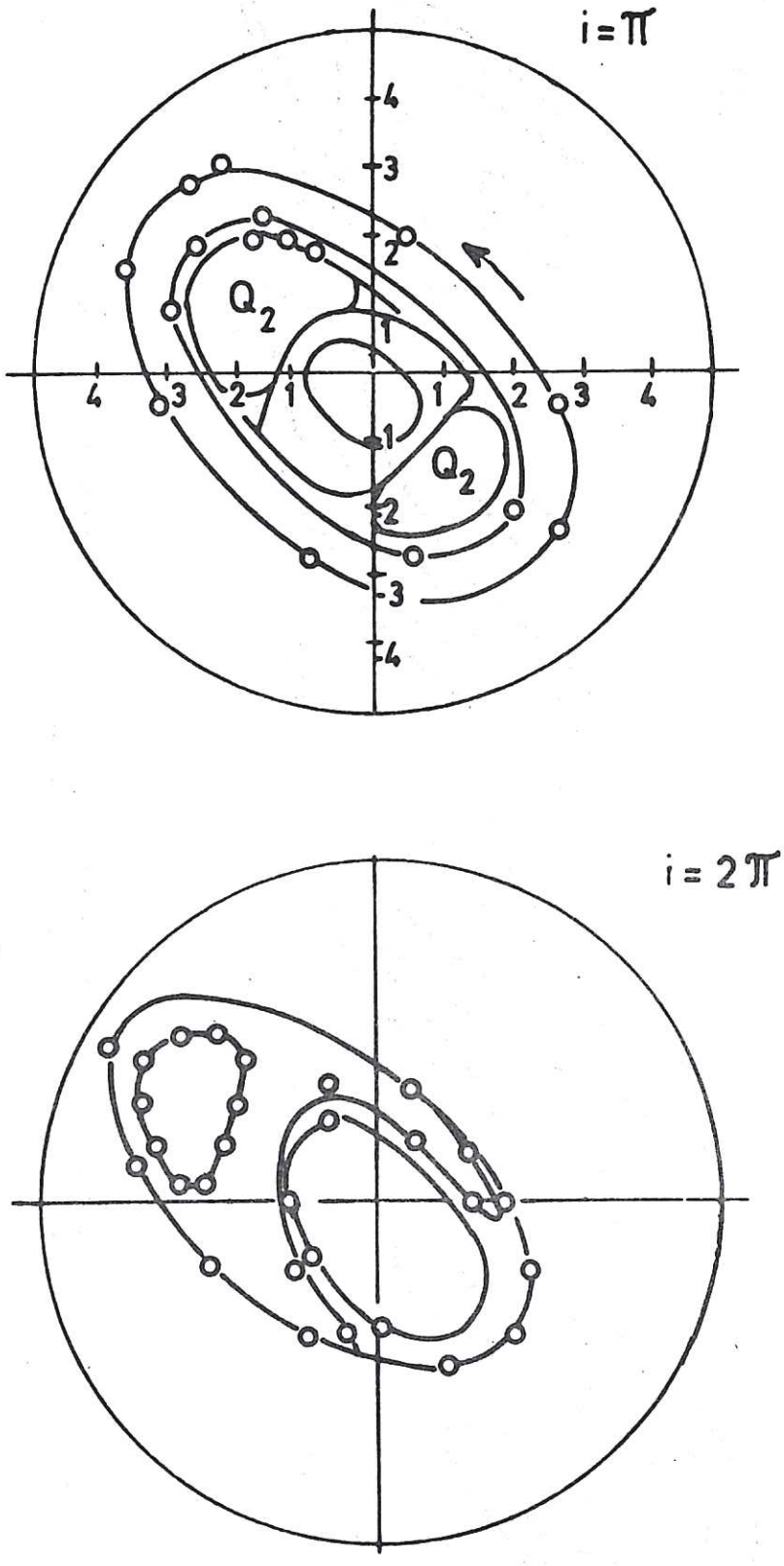

Fig.9 Resonance structure of the magnetic field on TOR-1 stellarator for $\iota = 0.5$ and 1.

CLM - R 142

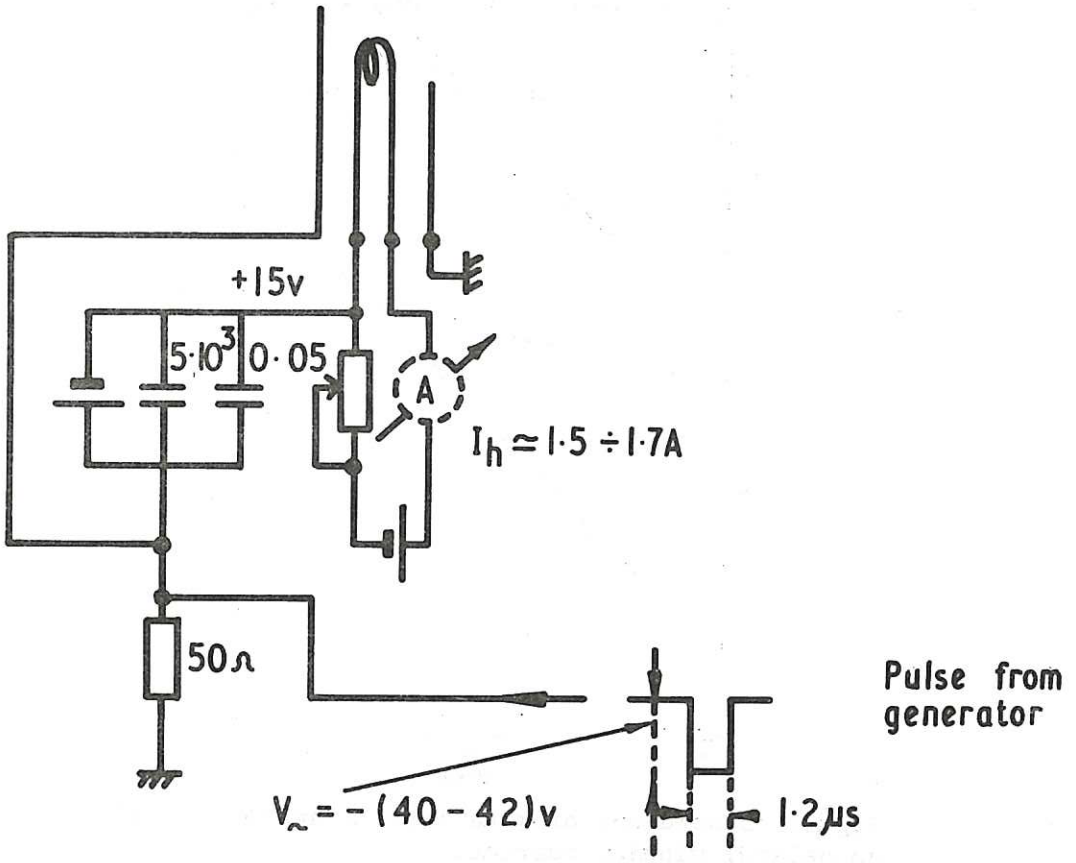

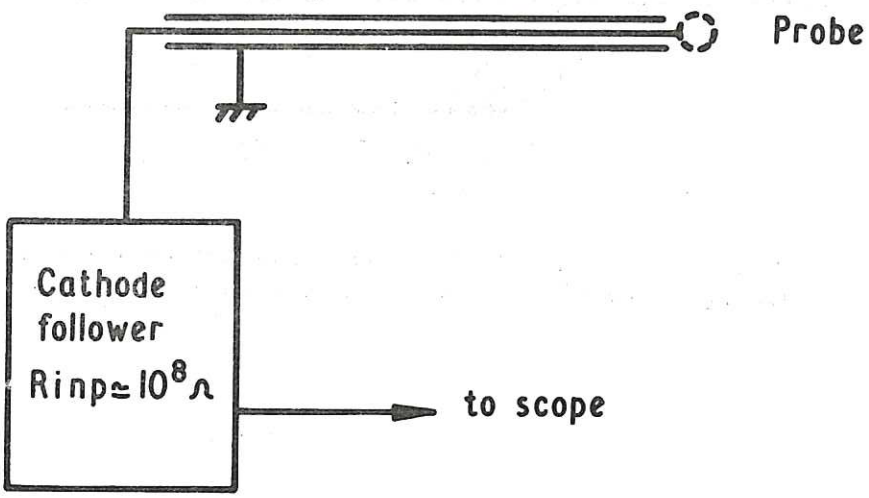

Fig.10 Schematic circuit for the power supply to the electron gun and the detector probe.

CLM - R 142

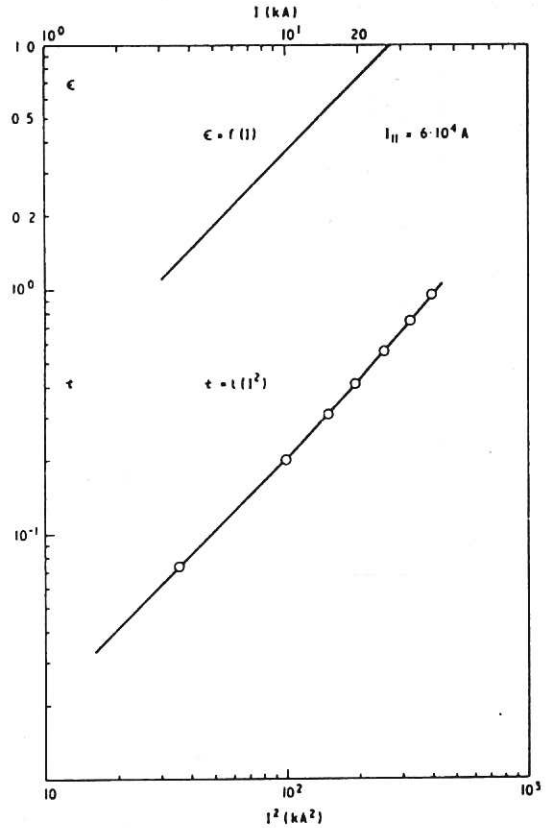

Fig.11 Dependence of rotational transferm ι and ϵ on helical winding current.

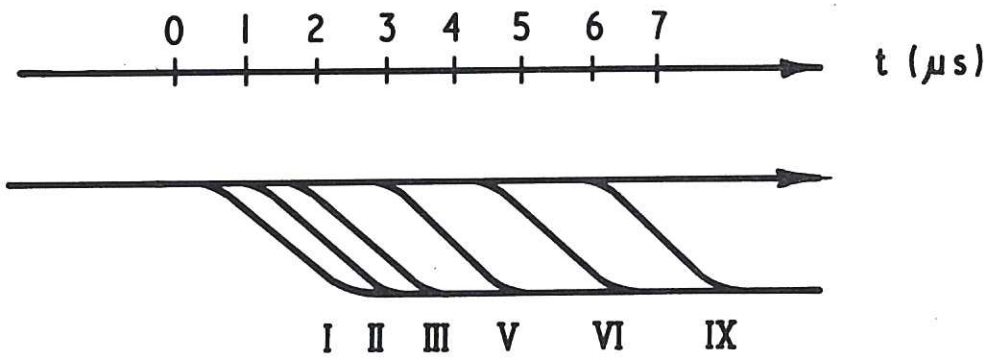

Fig.12 Oscillograms of signal from detector probe showing up to nine transits of the beam.

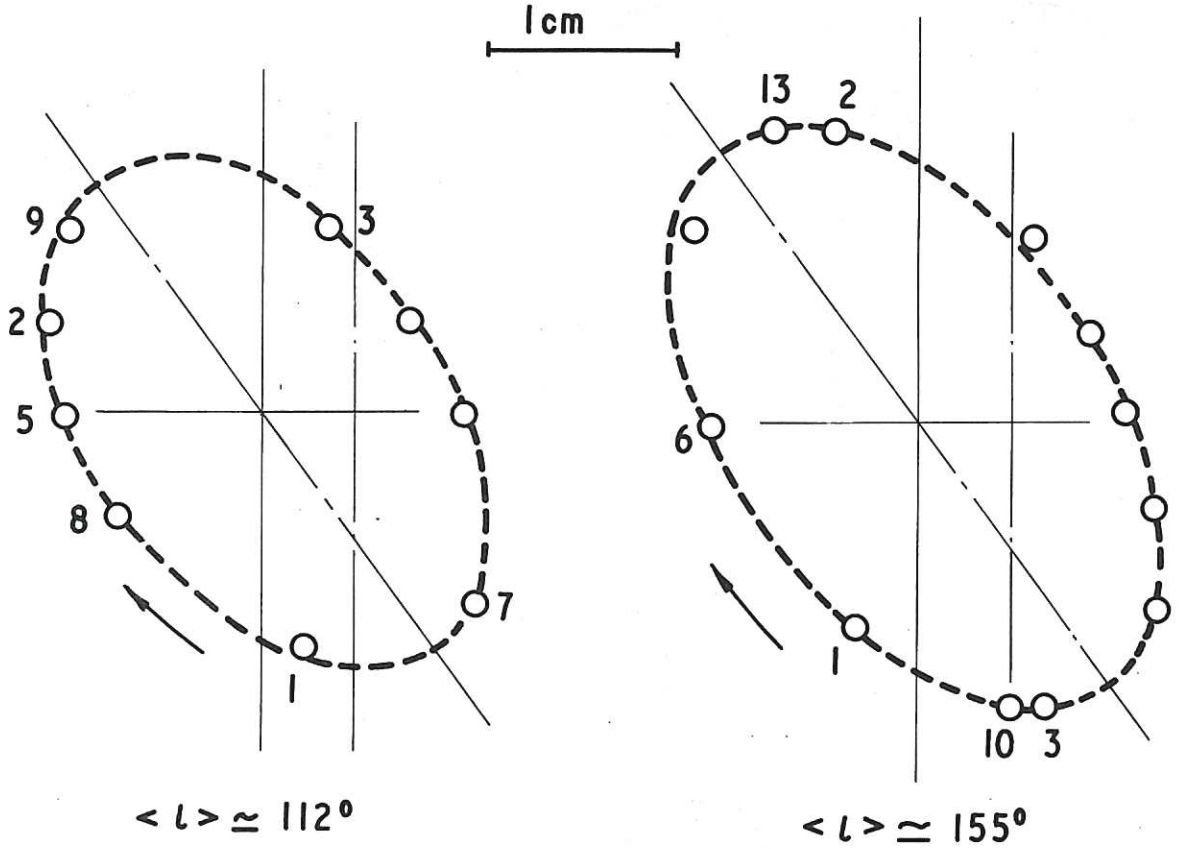

Fig.13 Some electron beam results for an inner surface. The number of transits of the beam and the average rotational transform for the surface are indicated.

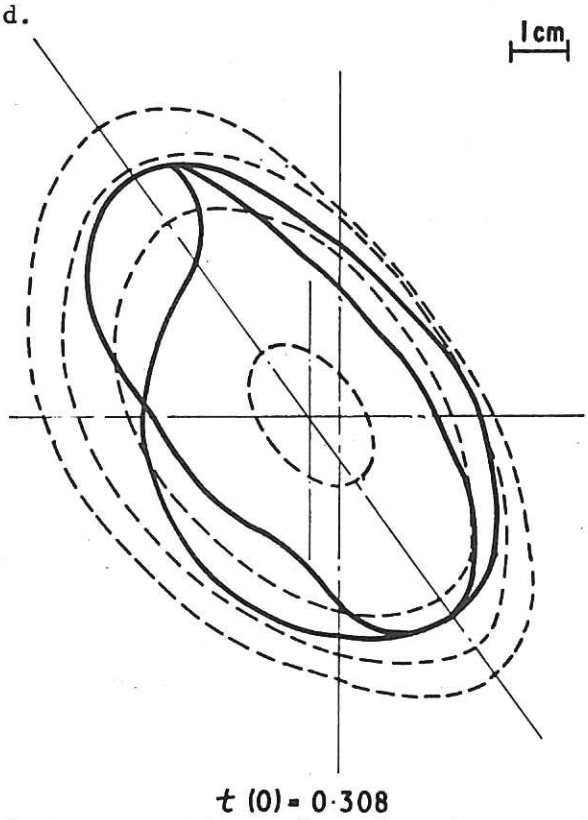

Fig.14 Outer magnetic surface for the case I_ℓ = 12 kA (ϵ = 0.445) showing the existence of a resonant perturbation structure of the third kind ($\iota = \frac{1}{3}$).

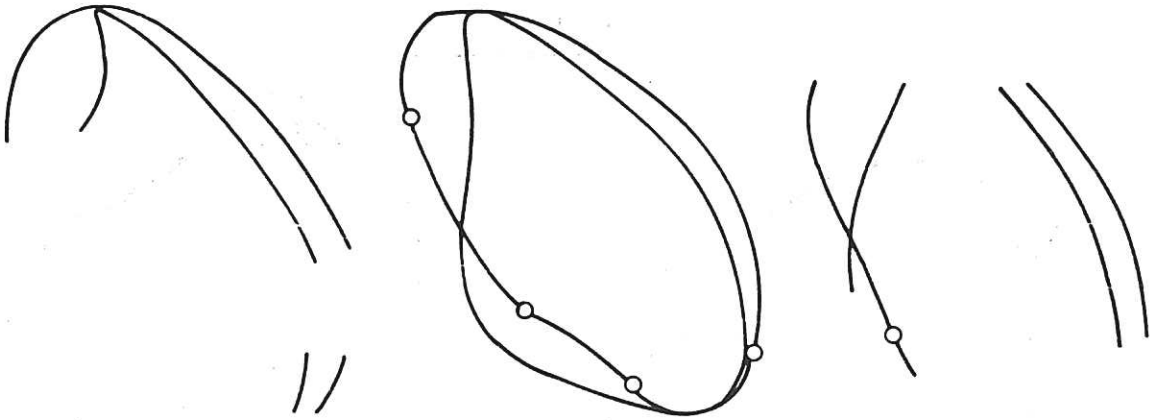

$t(0) = 0.308$

Fig.14a Outer magnetic surface for the case I_ℓ = 12 kA (ϵ = 0.445) showing the existence of a resonant perturbation structure of the third kind ($\iota = \frac{1}{3}$).

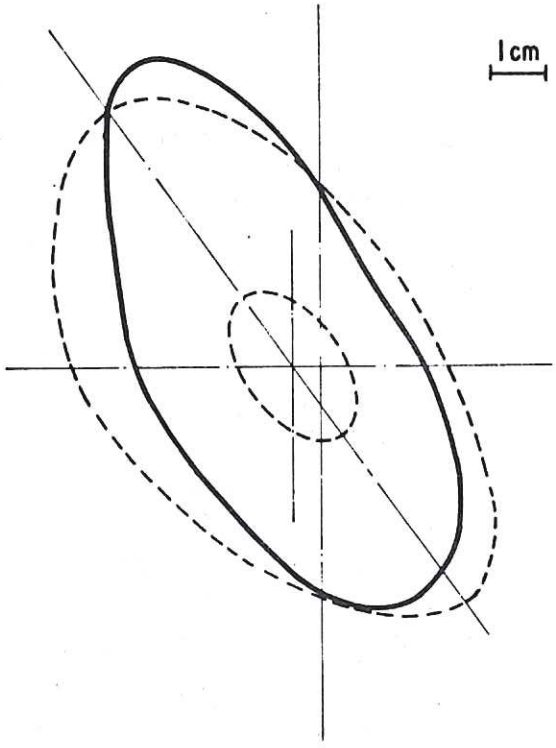

$t(0) = 0.43$

Fig.15 Outer magnetic surface for the case I_ℓ = 14 kA (ϵ = 0.518) showing resonance of the second kind ($\iota = 0.5$).

HER MAJESTY'S STATIONERY OFFICE

Government Bookshops

49 High Holborn, London WC1V 6HB
13a Castle Street, Edinburgh EH2 3AR
41 The Hayes, Cardiff CF1 1JW
Brazennose Street, Manchester M60 8AS
Wine Street, Bristol BS1 2BQ
258 Broad Street, Birmingham B1 2HE
80 Chichester Street, Belfast BT1 4JY

Government publications are also available through booksellers